AIAA '87

AIAA-87-0529
Validation of an Interior Noise Prediction Model for a Composite Cylinder

T.B. Beyer, NASA Langley Research Center, Hampton, VA: and F.W. Grosveld, The Bionetics Corp., Hampton, VA

AIAA 25th Aerospace Sciences Meeting
January 12-15, 1987/Reno, Nevada

VALIDATION OF AN INTERIOR NOISE PREDICTION MODEL FOR A COMPOSITE CYLINDER

Todd B. Beyer*
NASA Langley Research Center
Hampton, Virginia 23665-5225

Ferdinand W. Grosveldt
The Bionetics Corporation
Hampton, Virginia 23666

Abstract

An acoustic modal analysis has been performed in the cavity of a composite cylinder model of an aircraft fuselage. The filament wound, composite shell is 12 feet long and 5.5 feet in diameter. A one-half-inch thick plywood floor is attached to the shell 69 degrees from the vertical centerline through the bottom of the shell. The acoustic modal frequencies were obtained from a sound pressure level and phase survey conducted throughout the interior volume bounded by the floor, endcaps and stiffened shell, while being excited by white noise from a loudspeaker source. The measured acoustic resonance frequencies and mode shapes compare well with analytical predictions from the Propeller Aircraft Interior Noise (PAIN) model. Details of the theory and derivation of the acoustic characteristics have been included. Reverberation time measurements, using the integrated impulse technique, have been performed to determine acoustic loss factors. These measured loss factors have been input to the PAIN program in order to more accurately predict the space-averaged interior noise of the composite cylinder.

List of Symbols

$[A]$	matrix used to solve Helmholtz difference equation (equation 13)
a	cylinder radius
$C(j)$	factor used in acoustic mode normalization scheme (equation 18)
c_o	speed of sound in air
f_i	modal frequencies for cavity cross section
f_{qi}	modal frequencies for three-dimensional cavity
h	finite differences grid spacing, horizontal mode shape
k	wave number, $k = \omega/c_o$
L	cylinder length
l	longitudinal mode shape
n_j	number of interior and boundary points
$\{P_I\}$	column vector containing sound pressure levels at interior and boundary locations
$P_{m,n}$	sound pressure at grid location (x_m, y_n)
r	radial distance to finite difference grid location (x_m, y_n)
T_R	reverberation time
V	cavity volume
v	vertical mode shape
x,y,z	spatial coordinates
∇^2	Laplacian operator
ε_q	mode normalization factor for longitudinal mode
ε_{qi}	mode normalization factor for three-dimensional mode
η	acoustic loss factor
θ	angular coordinate
θ_{mn}	angular coordinate for grid location (x_m, y_n)
θ_o	angle at which shell/floor joint is located
λ_i	eigenvalue corresponding to mode shape ϕ_i
$\Phi_G(i)$	generalized mass for mode shape ϕ_i
ϕ_i	mode shape of the i^{th} mode of the cavity cross-section
ϕ_{qi}	mode shape (eigenfunction) of three-dimensional mode of cavity
ω	angular frequency

Subscripts

i	mode number counter for cross-section modes
j	counter over interior locations of cross-section (equation 16)
m,n	indices for grid locaton (x_m, y_n)
q	number of axial half-wavelengths

* Aerospace Engineer
† Aero-Space Research Engineer, Senior Member AIAA

Introduction

Passenger acceptance of new propeller aircraft, such as the advanced turboprop aircraft, is highly dependent on the control of interior noise levels. The application of composite materials to primary and secondary structures, combined with the high noise levels generated by advanced turboprops, have fostered the need for comprehensive theoretical and experimental acoustic research to fully examine and describe the acoustic behavior of this type of aircraft. One prediction method, the Propeller Aircraft Interior Noise (PAIN) model,[1] has recently been modified to permit the prediction of the space-averaged sound pressure levels inside fuselages constructed of laminated composites. As part of the Advanced Composites Structures Technology (ACST) program, a composite fuselage model has been designed and fabricated which will meet the design requirements of a 1990 large transport aircraft without substantial weight and cost penalties.[2,3] Some structural and acoustic characteristics of this laboratory model can be found in reference 4. The purpose of the present investigation is to determine experimentally the acoustic modal frequencies and loss factors of the composite cylinder with floor and compare them with values from the PAIN prediction model. A Computer Aided Test (CAT) system was used to

conduct a sound pressure level and phase survey of the enclosed volume while being subjected to random noise. This survey was used to determine the most dominant low-frequency (below 500 Hz) acoustic modes in the cavity, for comparison with those predicted by the PAIN program. The acoustic loss factors were determined using the integrated impulse method.

Propeller Aircraft Interior Noise Model

A computer program, entitled PAIN (Propeller Aircraft Interior Noise), has been developed for predicting the sound pressure levels inside propeller-driven aircraft.[1] The development, verification and application of this model can be found in references 5-13. The program calculates the space-averaged sound pressure levels inside the cabin space of an idealized fuselage at the propeller blade passage frequency and integral multiples of that frequency. The fuselage model consists of a cylinder stiffened by ring frames and stringers and a structurally integral floor. In the most recent version, the skin can be of a conventional homogeneous material (e.g. aluminum) or a laminated composite material. The interior surface of the cabin may be treated with a trim insulation and lining. The primary elements of the PAIN model are illustrated in Figure 1.

The PAIN model addresses the major factors that influence the sound field inside the cabin. The flow chart in Figure 2 outlines the basic sequence of the master PAIN program. The analysis requires a precise description of the exterior noise field (pressure amplitude and phase) which is defined over a grid that lies on the fuselage skin. This input data can be measured or predicted. For example, propeller data can be generated using a noise prediction program such as ANOPP (Aircraft Noise Prediction Program).[14] Structural modal properties (resonance frequencies and mode shapes) are calculated by the auxiliary programs MRP and MRPMOD. These programs require input data such as the cylinder geometry, the stiffener geometry and bending rigidities, the cylinder and floor masses per unit area and the location of the floor. The resonance frequencies and mode shapes for a two-dimensional cross-section of the acoustic space are calculated by the program CYL2D. The angle at which the floor is located must be input to this program. The output from these programs must be combined with additional input data related to the specific test specimen (structural and acoustic loss factors, sidewall trim characteristics, etc.) before a space-averaged sound pressure level inside the cylinder can be computed. If these characteristics are determined experimentally, the prediction model will more accurately describe the experimental situation.

Modal Properties of the Cabin Space

For a cylindrical cavity, the acoustic modal characteristics (resonance frequencies, mode shapes, etc.) can be determined in closed form by an analytical solution of the wave equation, subject to appropriate boundary conditions. This is possible because the wave equation is separable in cylindrical coordinates and the boundary conditions can be expressed in these coordinates. However, for the present case of a cylinder with a floor partition (Figure 1), the mode shapes cannot be derived in closed form because the boundary condition along the floor is difficult to express in cylindrical coordinates. Thus, a numerical method, either finite elements or finite differences, must be used to solve this problem. Since the endcap boundaries are parallel, the modal characteristics in the axial direction can be easily determined, and the problem can be reduced to a cross-sectional one. The finite difference technique is the simpler of the two numerical methods, and is used for the present case.

Finite Differences in Two Dimensions

Inside the cylinder, the volume bounded by the floor, endcaps and stiffened shell satisfies the Helmholtz equation. Thus, for the present cross-sectional problem

$$\nabla^2\phi + k^2\phi = 0 \tag{1}$$

where $\nabla^2 = \frac{\partial^2}{\partial x^2} + \frac{\partial^2}{\partial y^2}$ for rectangular coordinates. For the uniform grid shown in Figure 3, the central difference formula yields

$$\frac{\partial \phi_{mn}}{\partial x} = \frac{1}{2h}\left(P_{m+1,n} - P_{m-1,n}\right) \tag{2}$$

$$\frac{\partial \phi_{mn}}{\partial y} = \frac{1}{2h}\left(P_{m,n+1} - P_{m,n-1}\right) \tag{3}$$

$$\frac{\partial^2 \phi_{mn}}{\partial x^2} = \frac{1}{h^2}\left(P_{m+1,n} - 2P_{m,n} + P_{m-1,n}\right) \tag{4}$$

$$\frac{\partial^2 \phi_{mn}}{\partial y^2} = \frac{1}{h^2}\left(P_{m,n+1} - 2P_{m,n} + P_{m,n-1}\right) \tag{5}$$

where $\phi_{mn} = P_{m,n} = P(x_m, y_n)$ is the pressure and h is the grid spacing. Only half of the cylinder cross section is considered, since it is symmetric about x=0 (the vertical through the bottom of the cylinder). Substitution of these difference equations into equation (1) gives the Helmholtz equation in terms of finite differences,

$$4P_{m,n} - P_{m+1,n} - P_{m-1,n} - P_{m,n+1} - P_{m,n-1} = \lambda P_{m,n} \tag{6}$$

where $\lambda = k^2h^2$. This equation is valid for all points defined as interior (I) or boundary (B) points. Note that boundary points may lie inside or outside the cylinder, depending on which point of the grid lies closest to the cylinder (Figure 3). For each boundary point, exterior (E) points are required to solve the finite difference equation. The number of boundary conditions is equal to the number necessary to eliminate all of the exterior points.

The boundary condition requires that the outward normal gradient (velocity) is zero. This condition assumes that the wall admittance is

sufficiently small that it may be neglected. Thus, the shell boundary condition above the floor is

$$\left.\frac{\partial \phi}{\partial r}\right|_{\theta_o < \theta < \pi} = 0 \qquad (7)$$

For the geometry depicted in Figure 4

$$\frac{\partial x}{\partial r} = \sin\theta \qquad (8)$$

$$\frac{\partial y}{\partial r} = -\cos\theta \qquad (9)$$

Applying the chain rule to equation (7) yields

$$\frac{\partial \phi}{\partial r} = \frac{\partial \phi}{\partial x}\frac{\partial x}{\partial r} + \frac{\partial \phi}{\partial y}\frac{\partial y}{\partial r} = 0 \qquad (10)$$

Substitution of equations (8) and (9) and the difference equations (2) and (3) into equation (10) yields the boundary condition for the region $\theta_o < \theta < \pi$

$$(P_{m+1,n} - P_{m-1,n}) \sin\theta_{mn} = (P_{m,n+1} - P_{m,n-1}) \cos\theta_{mn} \qquad (11)$$

The boundary condition along the floor, $0 < \theta < \theta_o$ can be obtained from equation (11) by setting $\theta_{mn} = 0$ whenever $\theta_{mn} < \theta_o$. This yields

$$P_{m,n+1} = P_{m,n-1} \qquad (12)$$

The general solution can be represented in matrix notation as

$$[A]\{P_I\} = \lambda \{P_I\} \qquad (13)$$

where $\{P_I\}$ is the column vector containing the pressure at interior and boundary points. The matrix [A] is constructed such that the Helmholtz difference equation (6) and the boundary conditions (equations 11 and 12) will be satisfied. The eigenvalues and eigenvectors are calculated for symmetric and antisymmetric modes separately, and ranked in ascending order of frequency. The eigenvalue λ_i corresponds to the mode shape $\phi_i(x,y)$, where i is the two-dimensional mode counter. The resonance frequencies output by the program CYC2D are

$$f_i = \frac{c_o}{2\pi h}\sqrt{\lambda_i} \qquad (14)$$

where the radius a is normalized to one meter. The resonance frequencies for the three-dimensional space are given by

$$f_{qi} = \frac{c_o}{2\pi}\left[\left(\frac{q\pi}{L}\right)^2 + \left(\frac{\lambda_i}{h^2}\right)\right]^{1/2} \qquad (15)$$

The acoustic mode shapes for the three-dimensional space are given by the eigenvectors

$$\phi_{qi}(x,y,z) = \cos\left(\frac{q\pi}{L} z\right) \phi_i(x,y) = \cos\left(\frac{q\pi}{L} z\right) \phi_i(j) \qquad (16)$$

where $\phi_i(x,y) = \phi_i(j)$ is the two-dimensional mode calculated by the finite difference technique. The maximum value for any grid location is normalized to unity and the other values are scaled in order to maintain the original computed ratios. The acoustic mode normalization factor is

$$\varepsilon_{qi} = \frac{V}{\iiint \phi_{qi}^2 \, dv} \qquad (17)$$

The denominator of this expression can be expanded as

$$\iiint \phi_{qi}^2 \, dv = \left[\int_o^L \cos^2\left(\frac{q\pi}{L} z\right) dz\right] \sum_{Area} \phi_i^2 \, dArea$$

$$= \frac{L}{2}\varepsilon_q \sum_{j=1}^{n_j} \phi_i^2(j)\, h^2\, C(j) \qquad (18)$$

where j counts over all interior locations. The parameter C(j) equals 1 for boundary points and centerline (x=0) locations, while C(j) equals 2 for interior points. Also, $\varepsilon_q = 2$ for $q = 0$ and $\varepsilon_q = 1$ for $q > 0$. The generalized mass for mode i for a cylinder with unit radius, as output from the finite differences program, is

$$\Phi_G(i) = \sum_{j=1}^{n_j} \phi_i^2(j)\, h^2\, C(j) \qquad (19)$$

Composite Cylinder Test Article

The fuselage model used in the current study is a filament-wound stiffened cylinder 5.5 feet in diameter and 12 feet in length. The composite material for the shell of the cylinder consists of carbon fibers embedded in an epoxy resin. The ply-sequence of the cylinder's skin is $\pm 45, \pm 32, 90, \mp 32, \mp 45$ for a total thickness of 0.067 inch. The basic design of the stiffened cylinder includes 10 J-section ring frames and 22 evenly spaced hat-section stringers. A one-half-inch thick plywood floor, stiffened with aluminum I-beams, is installed 21.4 inches above the bottom of the cylinder. All elements of the cylinder are rivet-bonded together. Figure 4 shows a cross section of the floor-equipped cylinder with detail of the stringer-frame enforcement.

Impact testing was performed to determine important modal properties (resonance frequencies, mode shapes, etc.) of the structure for comparison with the analytical model.[4] Special endcaps were constructed from three layers of 1.25-inch thick particle board with a 0.125-inch wide groove routed out to support the cylinder. The endcaps are sufficiently massive so that any airborne sound transmission through them during acoustic testing is negligible compared to the sound transmission through the cylinder wall. The

entire structure is held together by four 0.50-inch diameter tension rods whose vibration resonances are effectively damped by specially designed wooden clamping devices. The spaces above and below the floor are acoustically isolated by rubber gaskets and silicon rubber sealant. Access to the interior of the cylinder is facilitated by a two-foot by two-foot hinged door. Acoustically sealed boxes, installed on the inside and outside of the front baffle, provide connections for microphones and electronic equipment.

Experimental Acoustic Analysis

In order to determine the important modal characteristics associated with the cylinder's interior acoustic space, sound pressure level and phase measurements have been conducted throughout the interior volume bounded by the floor, endcaps and stiffened shell. An I-beam located along the axis of the cylinder supports a boom on which six one-half-inch condenser microphones are mounted. A photograph of the microphone boom inside the cylinder is shown in Figure 5. The microphones are located at integral multiples of five inches from the centerline. One of the six microphones is positioned between the center beam and the floor. The microphone boom can be translated along the I-beam over the entire length of the cylinder and rotated through 220 degrees. In this manner, acoustic measurements can be obtained at different radial positions for any desired cross section.

Modal Frequencies

The interior of the cylinder was subjected to white noise from a loudspeaker source located in a corner where the floor meets the front endcap and the cylindrical shell. Frequency spectra, over the range 0 - 500 Hz (1Hz bandwidth), were obtained for each of the six microphones at 11 evenly spaced locations along the cylinder's length with the boom oriented in the vertical plane. Additional spectra were obtained for 15 radial locations with the boom positioned 11 feet from the cylinder's front endcap. Modal frequencies and mode shapes were identified from peak sound pressure levels in the frequency spectra and equal sound pressure level contour plots. Some of these measured mode shapes are shown in Figure 6. Adjacent contour lines represent a 3 dB change in root-mean-square sound pressure level. The heavy solid lines indicate the nodal lines of the measured acoustic mode shapes, where the root mean square pressure is a minimum and pressures on either side are out of phase.

To compare with the calculated modal frequencies equation 14 is substituted into equation 15

$$f_{qi} = \frac{c_o}{2\pi}\left[\left(\frac{q\pi}{L}\right)^2 + \left(\frac{2\pi f_i}{ac_o}\right)^2\right]^{1/2} \qquad (20)$$

where q is the longitudinal mode counter and f_i is the cross-sectional mode output from CYL2D. Good agreement has been obtained between experimental and calculated acoustic modal frequencies as evidenced by the results in Table I. The calculated acoustic mode shapes are projected onto the equal contour plots in Figure 6 (dashed lines) and compare well with the measured mode shapes. The lowest two modes (47 Hz and 94 Hz) are one-dimensional modes along the longitudinal dimension of the cylinder, having one and two nodal lines respectively. The sound pressure level for these modes does not vary significantly over the cross section. As the frequency increases the mode shapes become higher ordered and are more difficult to extract from the sound pressure level contour plots. An example is provided by the (4,0,1) mode at 249 Hz (Figure 8). Here the component of the mode in the cross section dominates the longitudinal component of the mode, which appears to be in transition between a mode with four nodal lines and one with five nodal lines. The projection of the calculated mode onto the sound pressure level contour plot helps resolve the mode.

The experimental setup did not allow for adequate measurement of acoustic modes which have a pressure minimum at or near the measurement locations. Due to weak modal response at these locations, these modes were not very well defined and have therefore not been included in Table I. Additional measurements, for other cross sections of the interior, are required to improve the resolution of these modes.

Acoustic Loss Factors

An important input parameter to the PAIN program is the band averaged acoustic loss factors. The acoustic loss factor of an enclosure can be calculated as a function of frequency and reverberation time

$$\eta = \frac{2.2}{f\,T_R} \qquad (21)$$

where the reverberation time, T_R, is defined as the time for the sound pressure level in an enclosure to decay through 60 dB. The usual method to measure the reverberation time is the interrupted noise method where the sound decay in the enclosure is recorded after filtered white noise is abruptly switched off. Since the noise source is random in nature, the noise at the instant of interruption is statistically uncertain, resulting in poor repeatability of the decay curves. It is impossible to make detailed investigations of the decay curves as irregularities are masked by random fluctuations. To obtain representative results, averaging of many measurements and the assurance of a wide dynamic range (35 dB) are necessary.

For the current study, the reverberation times of the enclosure were determined using the integrated impulse method. This technique does not require measurements over such a wide dynamic range and often aids in the detection of non-exponential decays. Basically, the method squares and integrates the response of an enclosure to a single impulse excitation, thereby obtaining a smooth decay curve which represents the ensemble average of the decay curves obtained using the standard reverberation technique. Additional

information and discussion of the integrated impulse method can be found in references 15 and 16.

The reverberation times for one-third octave bands up to and including the 500 Hz center frequency were measured using a reverberation processor based on the integrated impulse method. The microphone boom was positioned in a cross section 11 feet from the front endcap and measurements were obtained at six vertical and six horizontal microphone locations. The reverberation times were converted to acoustic loss factors using equation 21 and are tabulated in Table II. Also included in this table is the average acoustic loss factor over all the microphones for each appropriate frequency band. In the low-frequency region the acoustic loss factors are dependent on the presence of resonant modes within a frequency band. Those bands without resonant modes were found to have higher loss factors than those with only a few resonant modes. At higher frequencies, the modal density increases in successive frequency bands, and the acoustic loss factors decrease. The average acoustic loss factors are graphically depicted in Figure 7.

Interior Noise Prediction

Ongoing research is focused on the measurement and prediction of the noise reduction of the composite cylinder. To determine the noise reduction, the PAIN program requires information about the modal response of the structure and the acoustic space and the exterior noise source. The structural modal frequencies and mode shapes for the composite cylinder have been calculated previously and compare reasonably well with the measured characteristics.[4] Good agreement has been obtained for the measured and calculated acoustic modal frequencies and mode shapes. Structural damping and acoustic loss factors have been determined experimentally and have been entered into the PAIN program. An exponential horn was used as an exterior noise source, located three feet from the front endcap and one inch from the cylinder shell (Figure 8). The horn was driven at 183.5 Hz with an overtone at 367.0 Hz. The sound pressure level measured by the exterior microphone at these frequencies was 132.7 dB and 104.7 dB. The interior sound pressure level was measured by a microphone located in the corner where the floor meets the front endcap and the cylindrical shell (Figure 8). The measured noise reduction was 29.6 dB at 183.5 Hz and 20.9 dB at 367.0 Hz. the noise reductions calculated using the PAIN program were 21.3 dB and 10.5 dB. Several reasons may contribute to the discrepancies between measurement and prediction. The interior sound pressure level was measured by only one microphone and does not represent a space-averaged level. Small inaccuracies in the predictions of the structural and acoustic modes will change their coupling and affect the calculated interior noise levels. Finally, the noise reduction is dependent on the location of the exterior noise source and the distribution of the noise field over the cylinder's exterior. Research is continuing to verify noise reduction predictions by the PAIN program for this composite cylinder.

Concluding Remarks

An acoustic modal analysis has been performed in the cavity of a composite cylinder. The measured resonance frequencies and mode shapes have been compared with predictions from the Propeller Aircraft Interior Noise model. The resonance frequencies that were extracted from the measurements agree to within a few Hertz of the predicted frequencies. The mode shapes match reasonably well except for those where the microphones were positioned close to a nodal line. Additional measurements using different positions of the microphone boom should aid in identifying all remaining mode shapes. Acoustic loss factors were obtained from reverberation time measurements in the cavity using the integrated impulse technique. Frequency bands with few or no resonant modes had higher acoustic loss factors than frequency bands with higher modal densities. An average acoustic loss factor over all the microphone positions was computed which has been entered into the PAIN program to make interior noise predictions for this fuselage model.

References

[1] Pope, L. D.; Wilby, E. G.; and Wilby, J. F.: Propeller Aircraft Interior Noise Model. NASA CR-3813, July 1984.

[2] Jackson, A. C.: Transport Composite Fuselage Technology -- Impact Dynamics and Acoustic Transmission. Semi-annual Technical Report No. 2, NASI-17698, Lockheed-California Company, Burbank, CA, May 17, 1985.

[3] Jackson, A. C.: Transport Composite Fuselage Technology -- Impact Dynamics and Acoustic Transmission. Semi-annual Technical Report No. 3, NASI-17698, Lockheed-California, Burbank, CA, November 15, 1985.

[4] Grosveld, F. W.; and Beyer, T. B." Modal Characteristics of a Stiffened Composite Cylinder with Open and Closed End Conditions. AIAA Paper 86-1908, July 1986.

[5] Pope, L. D.; Rennison, D. C.; Willis, C. M.; and Mayes, W. H.: Development and Validation of Preliminary Analytical Models for Aircraft Interior Noise Prediction. Journal of Sound and Vibration, vol. 82, 1982, pp. 541-575.

[6] Pope, L. D.; Rennison, D. C.; and Wilby, E. G.: Analytical Prediction of the Interior Noise for Cylindrical Models of Aircraft Fuselages for Prescribed Exterior Noise Fields. Phase I: Development and Validation of Preliminary Analytical Models. NASA CR-159363, October 1980.

[7] Pope, L. D.; and Wilby, E. G.: Analytical Prediction of the Interior Noise for Cylindrical Models of Aircraft Fuselages for Prescribed Exterior Noise Fields. Phase II: Models for Sidewall Trim, Stiffened Structures, and Cabin Acoustics with Floor Partition. NASA CR-165869, April 1982.

[8] Wilby, E. G.; and Wilby, J. F.: Application of Stiffened Cylinder Analysis to ATP Interior Noise Studies. NASA CR-172384, August 1984.

[9]Pope, L. D.: Propeller Aircraft Interior Noise Model - Utilization Study and Validation. NASA CR-172428, September 1984.

[10]Wilby, E. G.; and Pope, L. D.: Propeller Aircraft Interior Noise Model - Users' Manual for Computer Program. NASA CR-172425, January 1985.

[11]Pope, L. D.; and Wilby, J. F.: Band-Limited Power Flow into Enclosures. Journal of the Acoustical Society of America, vol. 62, 1977, pp. 906-911.

[12]Pope, L. D.; and Wilby, J. F.: Band-Limited Power Flow into Enclosures. II. Journal of the Acoustical Society of America, vol. 67, 1980, pp. 823-826.

[13]Beyer, T. B., Powell, C. A.; Daniels, E. F.; and Pope, L. D.: Effects of Acoustic Treatment on the Interior Noise of a Twin-Engine Propeller Airplane. Journal of Aircraft, vol. 22, 1985, pp. 784-788.

[14]Zorumski, W. E.: Aircraft Noise Prediction Program Theoretical Manual. NASA TM 83199, 1981.

[15]Schroeder, M. R.: New Method of Measuring Reverberation Time. Journal of the Acoustical Society of America, vol. 37, 1965, pp. 409-412.

[16]Schroeder, M. R.: Response to "Comments on 'New Method of Measuring Reverberation Time'." Journal of the Acoustical Society of America, vol. 28, 1965, pp. 359-361.

TABLE I. MEASURED AND CALCULATED ACOUSTIC MODAL FREQUENCIES

Mode Shape l,h,v	Measured [Hz]	Calculated [Hz]
1,0,0	47	48
2,0,0	94	96
1,1,0	121	125
3,0,0	143	143
2,1,0	150	150
0,0,1	171	160
3,1,0	183	184
4,0,0	191	191
3,0,1	216	215
1,2,0	230	228
5,0,0	239	239
4,0,1	249	249
3,2,0	266	265
6,0,0	287	287
4,2,0	295	294
5,2,0	328	327
3,3,0	350	348
5,2,1	363	363

l-longitudinal, h-horizontal, v-vertical

TABLE II. ACOUSTIC LOSS FACTORS

One-Third Octave Band Center Frequency [Hz]	Microphone Position Along the Vertical Centerline 1	2	3	4	5	6	Modal Density	Microphone Position Along the Horizontal Centerline 1	2	3	4	5	6	Average Over All Microphone Positions
31.5	.107	.104	.104	.107	.103	.104	0	.106	.106	.104	.106	.104	.104	.105
40	.142	.141	.141	.141	.141	.116	0	.141	.140	.141	.142	.141	.116	.137
50	.035	.035	.036	.035	.046	.042	1	.036	.036	.036	.037	.044	.043	.038
63	.081	.078	.074	.066	.066	.080	0	.077	.077	.079	.071	.073	.080	.075
80	.084	.089	.100	.096	.137	.149	0	.073	.071	.073	.072	.092	.149	.099
100	.028	.027	.027	.028	.044	.045	2	.022	.021	.021	.021	.042	.044	.031
125	.054	.055	.062	.064	.064	.059	1	.035	.029	.026	.025	.048	.048	.047
160	.021	.018	.020	.021	.028	.032	4	.020	.021	.028	.037	.061	.058	.030
200	.012	.011	.015	.014	.016	.017	7	.014	.014	.015	.015	.023	.022	.017
250	.014	.014	.014	.014	.010	.009	11	.011	.009	.008	.009	.009	.009	.009
315	.008	.010	.009	.008	.016	.017	20	.008	.007	.008	.006	.010	.010	.017
400	.008	.006	.007	.006	.009	.010	28	.013	.009	.010	.011	.007	.009	.010
500	.008	.007	.008	.009	.008	.007	53	.007	.006	.006	.007	.007	.007	.007

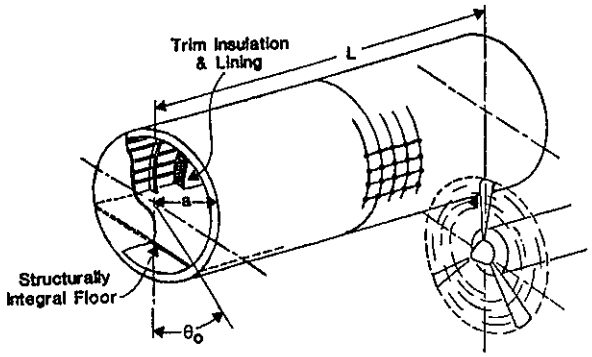

Fig. 1.- Elements of the Propeller Aircraft Interior Noise model.

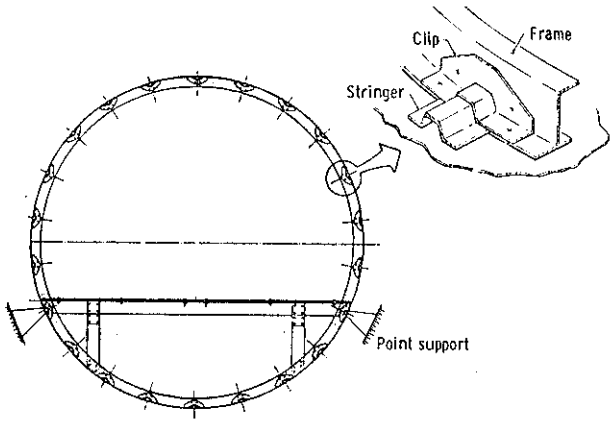

Fig. 4.- Cross section of composite stiffened cylinder with floor.

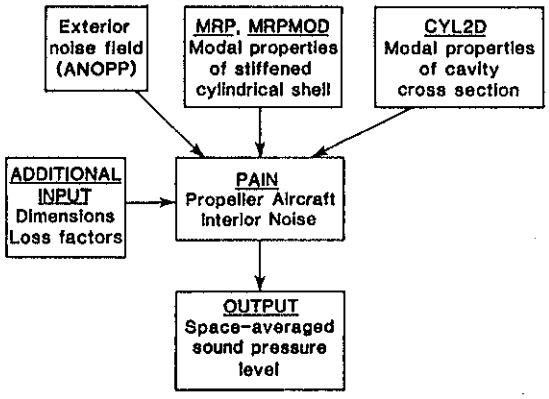

Fig. 2.- Flow chart of Propeller Aircraft Interior Noise computer program.

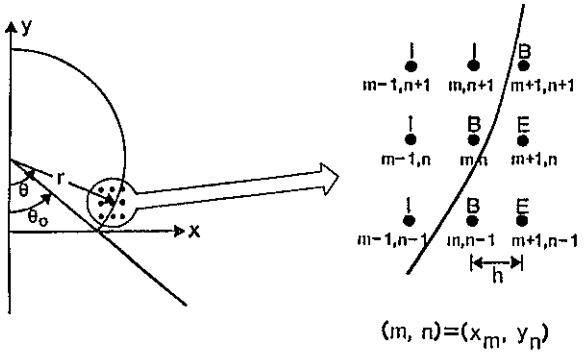

Fig. 3.- Geometry and nomenclature for finite differences scheme.

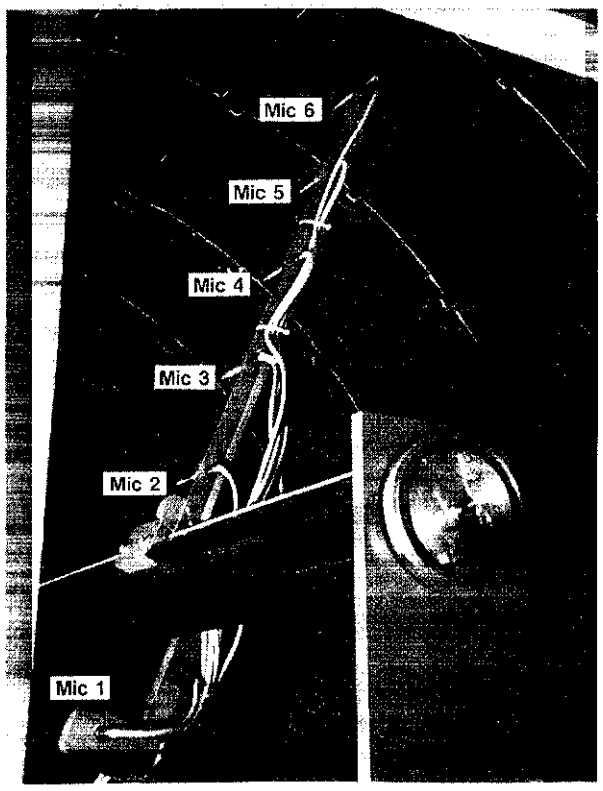

Fig. 5.- Microphone boom showing microphones used for interior noise survey.

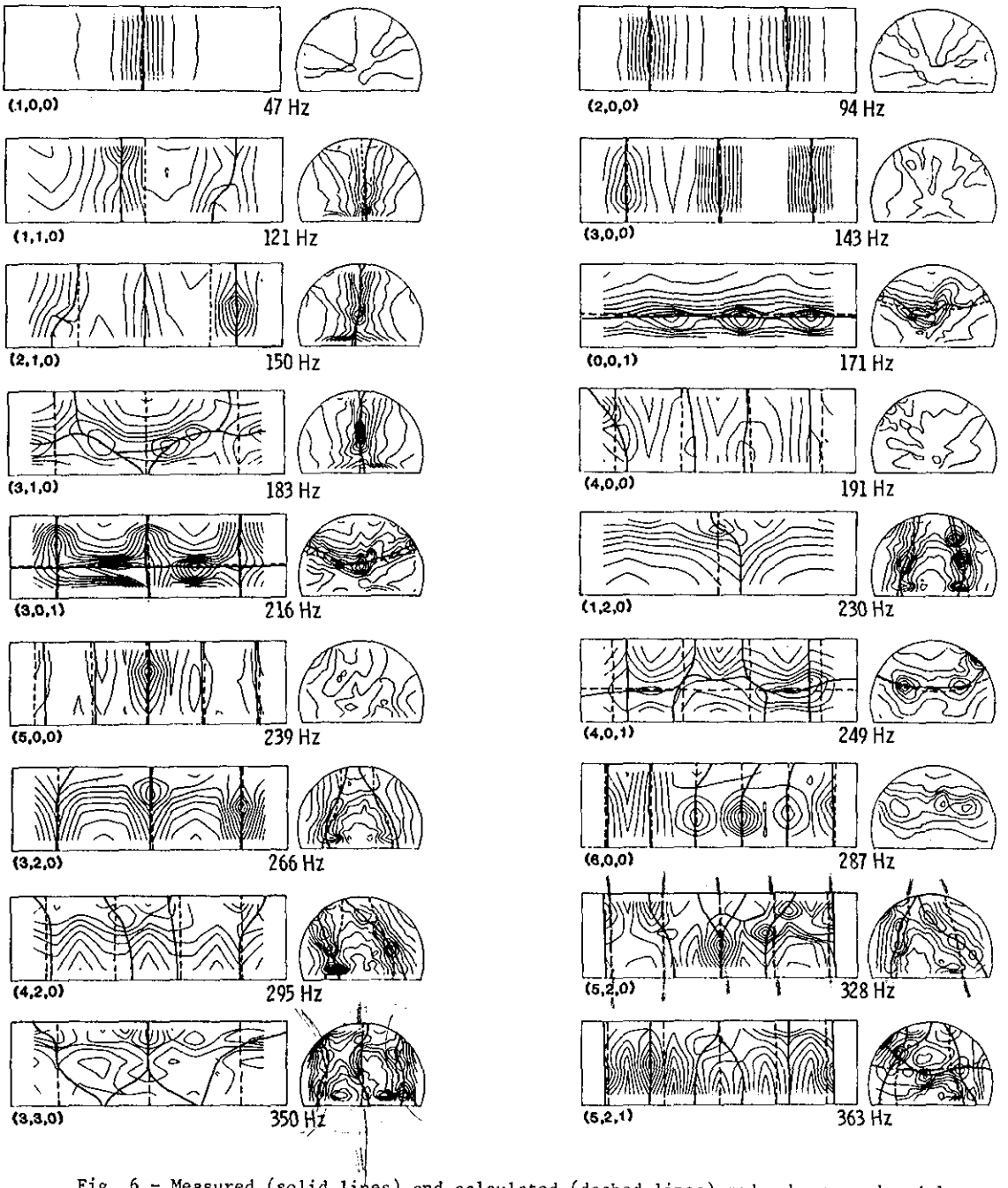

Fig. 6.- Measured (solid lines) and calculated (dashed lines) mode shapes and modal frequencies for cylinder cavity.

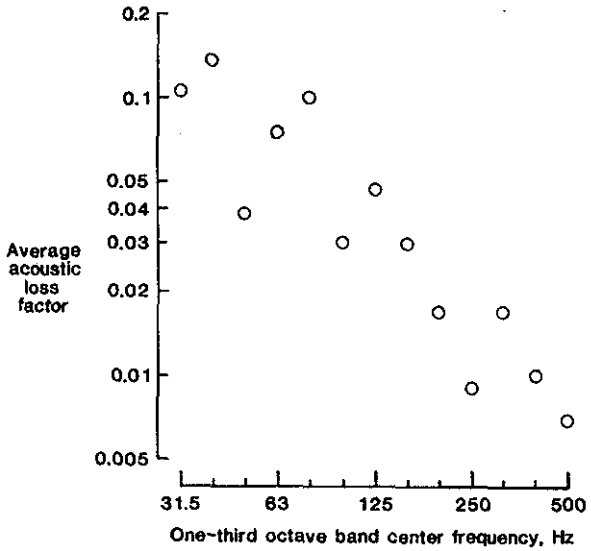

Fig. 7.- Average acoustic loss factor as function of one-third octave band center frequency.

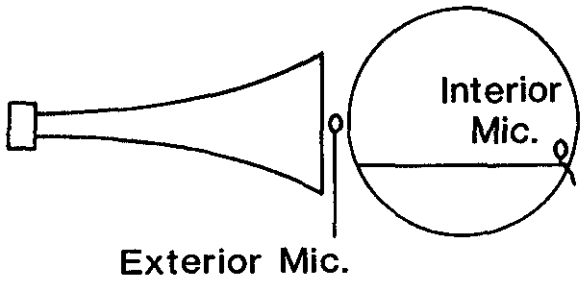

Fig. 8.- Experimental setup to measure noise reduction.